JCB Report

Recruitment of Eph receptors into signaling clusters does not require ephrin contact

Sabine H. Wimmer-Kleikamp,[1] Peter W. Janes,[2] Anthony Squire,[3] Philippe I.H. Bastiaens,[3] and Martin Lackmann[1]

[1]Ludwig Institute for Cancer Research, Royal Melbourne Hospital, Parkville, Victoria 3050, Australia
[2]Department of Biochemistry and Molecular Biology, Monash University, Clayton, Victoria 3800, Australia
[3]European Molecular Biology Laboratory, 69117 Heidelberg, Germany

Eph receptors and their cell membrane–bound ephrin ligands regulate cell positioning and thereby establish or stabilize patterns of cellular organization. Although it is recognized that ephrin clustering is essential for Eph function, mechanisms that relay information of ephrin density into cell biological responses are poorly understood. We demonstrate by confocal time-lapse and fluorescence resonance energy transfer microscopy that within minutes of binding ephrin-A5–coated beads, EphA3 receptors assemble into large clusters. While remaining positioned around the site of ephrin contact, Eph clusters exceed the size of the interacting ephrin surface severalfold. EphA3 mutants with compromised ephrin-binding capacity, which alone are incapable of cluster formation or phosphorylation, are recruited effectively and become phosphorylated when coexpressed with a functional receptor. Our findings reveal consecutive initiation of ephrin-facilitated Eph clustering and cluster propagation, the latter of which is independent of ephrin contacts and cytosolic Eph signaling functions but involves direct Eph–Eph interactions.

Introduction

Eph receptor tyrosine kinases (Ephs) and ephrins are essential cell surface–bound cell guidance cues acting during vertebrate embryogenesis (Flanagan and Vanderhaeghen, 1998; Holder and Klein, 1999). They are suggested as graded molecular tags that monitor the abundance or density of their reaction partner on opposing cells and relay this information to elicit correspondingly graded cellular responses. In contrast to other receptor tyrosine kinases, Eph receptor activation does not only require ligand binding and dimerization but also relies on preformed ligand oligomers. Thus, tyrosine phosphorylation of Eph receptors requires presentation of ephrin ligands in either clustered or membrane-attached forms (Davis et al., 1994), and other functional and biochemical Eph responses occur only at higher ligand oligomerization states (Stein et al., 1998).

Important structural and mechanistic insights into the initiation of Eph/ephrin signaling are provided by the X-ray structure of the complexed EphB2–ephrin-B2 interaction domains (Himanen et al., 2001). Ephs and ephrins combine into a circular 2:2 heterotetramer, held together by Eph–ephrin heterodimerization and heterotetramerization interfaces (Himanen et al., 2001; Himanen and Nikolov, 2003). In the model structure, the COOH termini of Eph and ephrin domains are positioned to opposite sites of the crystal plane, in agreement with an orientation of receptors and ligands on juxtaposed cells to enable bidirectional signaling. Recently, we confirmed through analysis of EphA3 point mutants with impaired ephrin-A5 binding that the protein interfaces predicted from the EphB2–ephrin-B2 crystal structure are also essential for the assembly of signaling-competent EphA3–ephrin-A5 complexes (Smith et al., 2003).

We have now used GFP fusion proteins of wild-type (w/t) EphA3 and ephrin binding–impaired mutants, together with signaling-compromised EphA3 receptors harboring mutations in their cytoplasmic domains, to examine ephrin-induced Eph receptor clustering by confocal time-lapse and

The online version of this article includes supplemental material.

Address correspondence to Martin Lackmann, Dept. of Biochemistry and Molecular Biology, P.O. Box 13D, Monash University, Clayton, Victoria 3800, Australia. Tel.: 61 3 9905 3738. Fax: 61 3 9905 3726. email: Martin.Lackmann@med.monash.edu.au

S.H. Wimmer-Kleikamp and M. Lackmann's present address is Dept. of Biochemistry and Molecular Biology, Monash University, Clayton, Victoria 3800, Australia.

Key words: fluorescence resonance energy transfer microscopy; EphA3 receptor; receptor protein tyrosine kinase; receptor aggregation; signal transduction

Abbreviations used in this paper: 3YF EphA3, [Tyr_{596}-Phe, Tyr_{602}-Phe, Tyr_{779}-Phe] EphA3; Ephs, Eph receptor tyrosine kinases; FLIM, fluorescence lifetime imaging microscopy; FRET, fluorescence resonance energy transfer; HEK293, human epithelial kidney 293; nb-EphA3, [Phe_{152}-Leu, Val_{133}-Glu] EphA3; w/t, wild-type.

The Journal of Cell Biology, Volume 164, Number 5, March 1, 2004 661–666
http://www.jcb.org/cgi/doi/10.1083/jcb.200312001

The Journal of Cell Biology

fluorescence resonance energy transfer (FRET) microscopy. FRET microscopy, based on measurable energy transfer between closely located donor and acceptor fluorophores (Bastiaens and Pepperkok, 2000; Wouters et al., 2001), monitors protein–protein interactions in situ and recently allowed elucidation of lateral signal transduction mechanisms of the EGF receptor (Reynolds et al., 2003). Here, we elucidate the mechanism leading to the assembly of extensive Eph receptor signaling clusters to cell membrane areas of ephrin contact. Our discovery of ephrin-independent recruitment of Ephs, including ephrin-binding or signaling compromised receptors, into nascent Eph–ephrin clusters has important consequences for the regulation of Eph/ephrin functions and for understanding intercellular communication mechanisms that are based on cell contact–mediated receptor clustering.

Results and discussion

Multivalent ephrin-A5-Fc is drawn into large cell membrane clusters and internalized into EphA3-expressing cells

The use of fluorescent ephrin-A5-Fc derivatives (Alexa ephrinA5-Fc) allowed us to monitor for the first time in real-time the rapid formation of Eph–ephrin signaling clusters by confocal time-lapse microscopy (Video 1, available at http://www.jcb.org/cgi/content/full/jcb.200312001/DC1). Exposure of EphA3-expressing cells to preclustered Alexa ephrin-A5-Fc resulted in rapid appearance of fluorescent patches on the cell surface, accumulating within 5 min into extensively stained cell surface ephrin clusters (Fig. 1 A, 10', arrowheads) indicative of rapid assembly of higher-order Eph–ephrin complexes. Within 35 min, small fluorescent vesicles moved from the cytoplasmic membrane side of the more prominent clusters (Video 1) into the cytosol, and analysis of Lysotracker green–stained EphA3/293 cells confirmed colocalization of the internalized Alexa ephrin-A5-Fc with lysosomal vesicles (Fig. 1 C, 35' and 90', yellow staining in the merged red [Alexa ephrinA5-Fc] and Lysotracker green images). Clustering and internalization was marginal with nonclustered Alexa ephrin-A5-Fc (Fig. 1 A; and Fig. 1 B, I and III) and was not abrogated in the presence of excess human IgG to block potential Fc receptor–mediated uptake (Fig. 1 B, II), suggesting an Fc receptor–independent endocytosis mechanism that concurs with EphA3 activation.

Multivalent ephrin-A5 triggers the assembly of large EphA3 receptor signaling clusters

We engineered a chimeric COOH-terminal EphA3/GFP fusion protein to measure EphA3 phosphorylation and clustering within cells by FRET using a CY3-conjugated antiphosphotyrosine monoclonal antibody (PY72) as the fluorescence acceptor (Bastiaens and Pepperkok, 2000; Wouters et al., 2001). Expression of the EphA3–GFP fusion construct was apparent on the plasma membranes of transiently transfected human epithelial kidney 293 (HEK293) cells and inside intracellular pools (Fig. 2, A–C, left). In the absence of ephrin-A5-Fc, phase or modulation lifetimes of the GFP fluorescence did not change, indicating the absence of FRET, and thus undetectable Eph receptor autophosphorylation in these

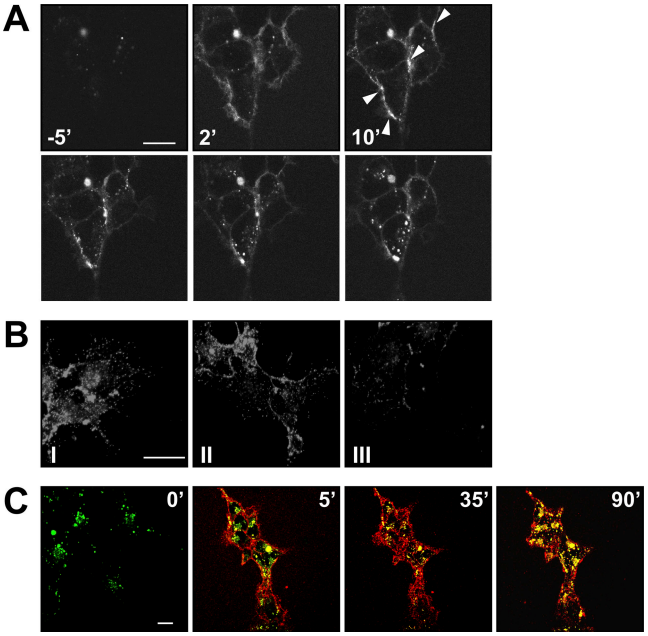

Figure 1. **The dynamics of ephrin-A5 clustering and internalization.** (A) Confocal time-lapse microscopy of ephrin binding and clustering. Preclustered Alexa ephrin-A5Fc was added to EphA3/293 cells and confocal microscopic images of live cells during a 60 min time course were taken every minute starting 5 min before ephrin addition. Arrowheads highlight prominent ephrin cluster. A corresponding Video 1 is available at http://www.jcb.org/cgi/content/full/jcb.200312001/DC1. (B) EphA3/293 cells were treated with preclustered Alexa ephrin-A5Fc in the absence (I) or in the presence (II) of "Fc block," or with nonclustered Alexa ephrin-A5Fc (III). After 30-min incubation, fixed cells were analyzed by confocal fluorescence microscopy. (C) Before stimulation with preclustered Alexa ephrin-A5Fc, the lysosomal compartment of EphA3/293 cells was stained with Lysotracker green. Alexa ephrin-A5Fc internalization was monitored sequentially at two excitation wavelengths. Resulting green (Lysotracker) and red (Alexa Fluor 546) images were merged. Bars, 20 μm.

EphA3-overexpressing cells (Fig. 2 A). However, challenge with preclustered (Fig. 2 C), but not with nonclustered, ephrin-A5-Fc (Fig. 2 B) induced a prominent reduction of GFP fluorescence lifetimes in distinct patches that was accompanied by pronounced cell rounding, suggesting that FRET microscopy provides a reliable measure of EphA3 phosphorylation and downstream responses (Fig. 2, B and C).

To examine the specificity of FRET microscopy in the context of Eph/ephrin signaling, we monitored EphA3 GFP fluorescence lifetime changes after pervanadate inhibition of cytosolic tyrosine phosphatase activity to achieve global activation of tyrosine kinases. In w/t EphA3GFP-expressing cells, this resulted in a concentration-dependent EphA3GFP lifetime reduction spreading across the whole cell surface (Fig. 2 C). In contrast, in cells expressing a mutant EphA3GFP that lacks the juxta-membrane and activation loop tyrosines ([Tyr_{596}-Phe, Tyr_{602}-Phe, Tyr_{779}-Phe] EphA3; 3YF EphA3GFP; Lawrenson et al., 2002), no measurable change in the EphA3GFP lifetime was apparent (Fig. 2 D), confirming that the FRET signal is specific for phosphorylated EphA3. In addition, this finding verifies the three tyrosines mutated in 3YF EphA3GFP as principle

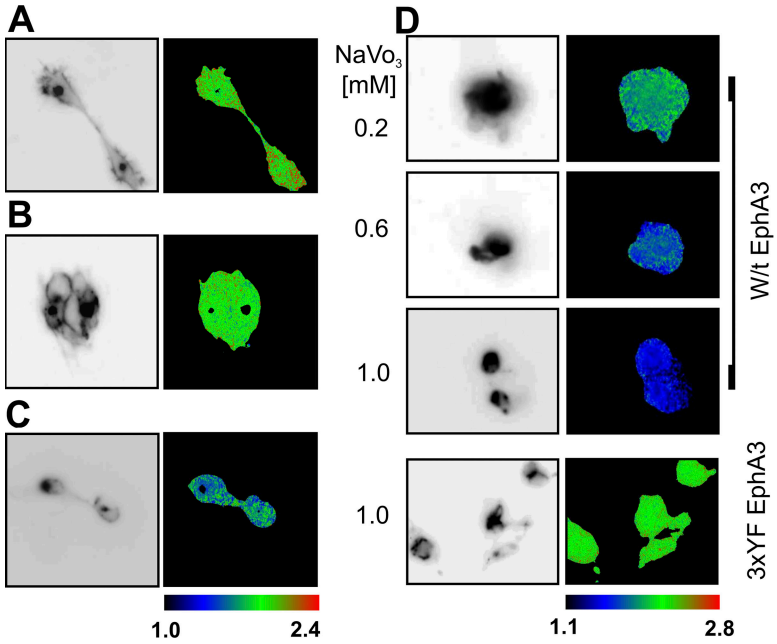

Figure 2. **Ephrin-A5 induced assembly of EphA3 signaling clusters.** (A–C) EphA3-GFP transfected HEK293cells, unstimulated (A) or stimulated (30 min) with soluble (B) or preclustered ephrin-A5Fc (C) were fixed, permeabilized (0.1% Triton-X 100), and incubated with CY3-PY72. The GFP fluorescence is shown as inverted gray scale (left). FRET between EphA3GFP and CY3-PY72 was detected by FLIM, and phase lifetime maps (right) are shown. "Blacked-out" areas within the lifetime maps mask regions that were excluded from FLIM analysis. They include areas within cells where high GFP fluorescence intensity resulted in saturated detection. (D) Pervanadate-induced Eph receptor phosphorylation. HEK293 cells expressing w/t EphA3GFP or 3YF EphA3GFP were incubated with pervanadate (30 min) at the indicated concentrations. Fixed cells were examined for FRET as described in A–C. Left, GFP fluorescence; right, GFP fluorescence lifetime phase maps. Tabulated color codes (dark blue to red) indicate GFP lifetimes in nanoseconds.

EphA3 phosphorylation sites. Also, dose-dependent EphA3 phosphorylation by pervanadate treatment of cells suggests that, similar to growth factor receptor tyrosine kinases (Ostman and Bohmer, 2001), basal EphA3 phosphorylation levels are regulated by protein tyrosine phosphatase activity.

EphA3 signaling clusters extend beyond direct receptor–ligand contacts

To examine the extent of direct EphA3–ephrin contacts, we monitored, by FRET microscopy, interactions between a chimeric GFP/ephrin-A2 protein (Hattori et al., 2000), as a fluorescence donor, and Alexa546-labeled EphA3Fc, as a fluorescence acceptor. We, and others, demonstrated previously that ephrin-A2 and ephrin-A5 bind EphA3 with very similar affinities (Lackmann et al., 1997; Flanagan and Vanderhaeghen, 1998), and it is well documented that both ephrins fulfill similar, if not identical, cell biological functions in vivo (Klein, 1999). Stimulation of GFP/Ephrin-A2–expressing cells with Alexa EphA3–coated beads resulted within minutes in a distinct reduction in GFP lifetime, strictly confined to the bead–cell interface (Fig. 3 A and Fig. S1, arrowheads depict the location of the bead, available at http://www.jcb.org/cgi/content/full/jcb.200312001/DC1).

Next, we examined in a similar approach EphA3 clustering and phosphorylation by using ephrin-A5-Fc–coated beads to activate cell surface EphA3 GFP. The phosphorylated receptor, identified in the microscopic images as areas of reduced GFP lifetime (Fig. 3 B, III) and as population of active receptors (Fig. 3 B, IV), accumulated into distinct clusters within the immediate vicinity of the contacting biobeads, but in addition spread over an extensive but locally defined surrounding area (Fig. 3 B, III and IV, arrowheads indicate the location of beads). We verified the authenticity of the fluorescence energy transfer observed in this experiment by photobleaching of the fluorescent acceptor CY3-PY72 in a control sample, abrogating any change in GFP lifetimes (Fig. S2 A, available at http://www.jcb.org/cgi/content/full/jcb.200312001/DC1).

A comparison of the clustering events observed either by monitoring Eph–ephrin complexes on the cell membrane (Fig. 3 A) or by imaging phosphorylated receptors on its cytoplasmic side (Fig. 3 B) suggested that binding of ephrin-A5-Fc beads triggers formation and propagation of activated (phosphorylated) EphA3 clusters that dramat-

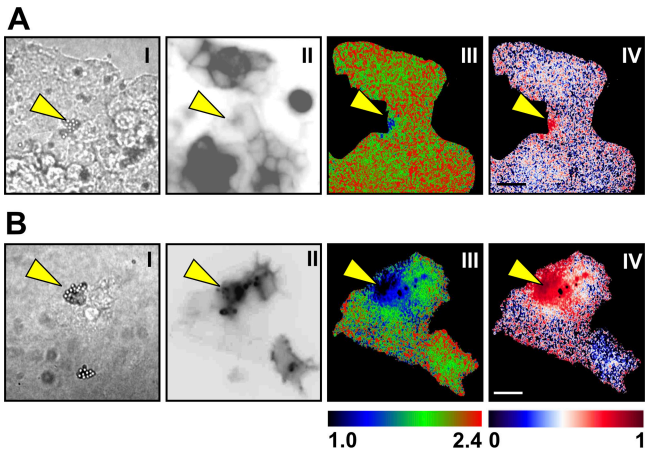

Figure 3. **EphA3 signaling clusters extend beyond ephrin contact surfaces.** (A) GFP ephrin-A2–expressing HEK293 cells were stimulated with Alexa EphA3-Fc–coated beads. The GFP ephrin-A2 and Alexa EphA3-Fc populations in contact were monitored by FLIM. Transmitted light (I), GFP fluorescence (II), phase lifetime maps (III), and the fraction (population) of ephrin-A2 in contact with Alexa EphA3-Fc (IV) are presented. Bar, 20 μm. (B) EphA3-GFP–expressing HEK293 cells were stimulated with ephrin-A5–coated beads and processed as described in Fig. 2. Images of transmitted light (I), GFP fluorescence (II), phase lifetime maps (III), and the fraction (population) of phosphorylated EphA3 (IV) are shown. Bar, 20 μm. (A and B) Tabulated color codes indicate GFP lifetimes in nanoseconds (III) and probabilities of phosphorylated EphA3GFP (IV). Arrowheads indicate the position of ephrin-coated beads.

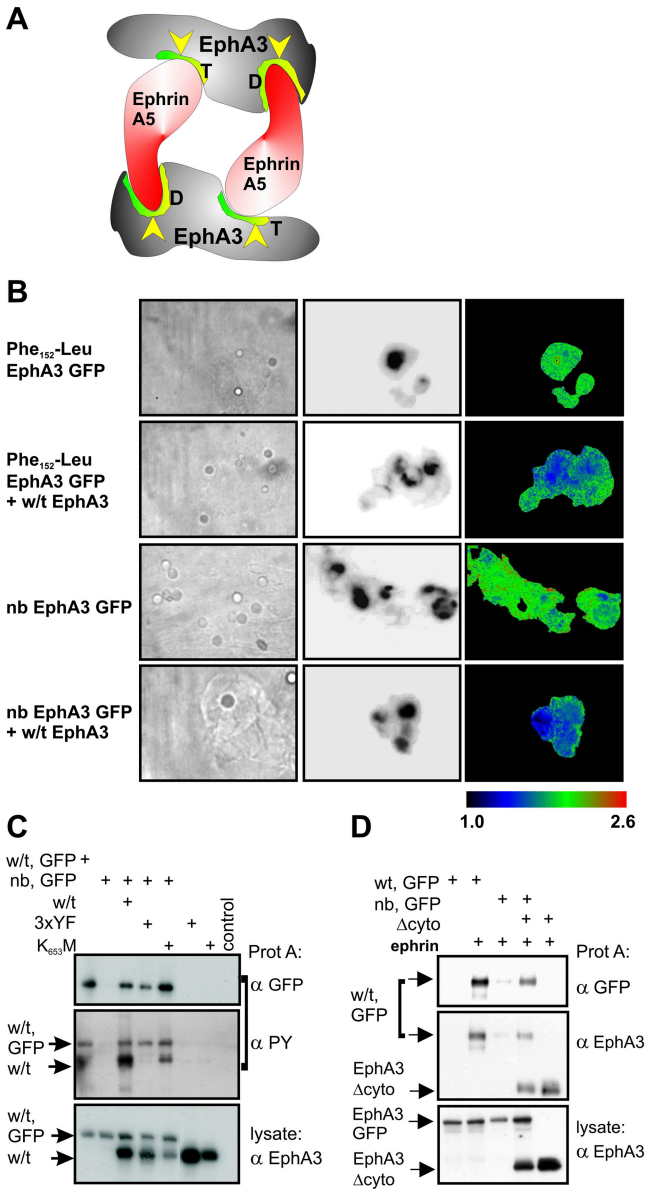

Figure 4. **Recruitment of EphA3 into signaling clusters is independent of direct ephrin contact.** (A) Model of the complex between Eph and ephrin binding domains, illustrating amino acid substitutions that affect ephrin binding. The cartoon is derived from the crystal structure of the EphB2/ephrin-B2 binding domains (Himanen et al., 2001). EphA3 interfaces in the putative heterodimerization (D) and heterotetramerization sites (T) that are involved in ephrin-A5 interactions as assessed by mutagenesis analysis (Smith et al., 2003) are indicated by yellow/green shading. The positions of two ephrin-binding point mutations in nb-EphA3 are indicated by yellow arrowheads. (B) HEK293cells, transfected either with [Phe_{152}-Leu] EphA3GFP or nb-EphA3-GFP alone, or in combination with unlabeled w/t EphA3 as indicated were stimulated with ephrin-A5Fc beads, and fixed cells were analyzed for FRET between the donor GFP and CY3-PY72 as described in Fig. 2. Transmitted light (left), GFP fluorescence (middle), and phase lifetime maps (right) are shown. (C) HEK293 cells were transfected, alone or in combination, with nb-EphA3-GFP or with untagged w/t EphA3, 3YFEphA3, or $K_{653}M$ EphA3 as indicated. After stimulation, protein A–bound EphA3 signaling complexes were analyzed with anti-GFP (α GFP, top) and antiphosphotyrosine (α PY, middle) antibodies. Total cell lysates were probed with anti-EphA3 antibodies to assess comparative expression levels (α EphA3, bottom). Irrelevant lanes have been removed from the Western blot. (D) HEK293 cells transfected, alone or in combination, with nb-EphA3-GFP and EphA3Δcyto. Protein A–bound complexes, recovered as in Fig. 4 C, were analyzed with anti-GFP (top) and anti-EphA3 antibodies (middle). Lysates were analyzed for EphA3 expression levels (bottom).

ically exceed the size of ligand and receptor populations in direct contact.

Recruitment of ephrin-binding impaired receptors into signaling clusters

To examine this apparent recruitment of new Eph receptors into existing Eph–ephrin signaling clusters we used ephrin-binding impaired mutants of EphA3GFP, containing amino acid substitutions in both the ephrin heterodimerization and heterotetramerization (Himanen et al., 2001) sites, [Phe_{152}-Leu, Val_{133}-Glu] EphA3 (nb-EphA3-GFP), or in the heterodimerization site alone, [Phe_{152}-Leu] EphA3GFP (Fig. 4 A). Recently, we demonstrated that these point mutations severely affect ephrin-A5 binding and abrogate EphA3 signaling (Smith et al., 2003). As expected, stimulation with ephrin-A5-Fc beads of cells expressing these EphA3 mutants did not yield a measurable change in GFP fluorescence lifetimes (Fig. 4 B). Intriguingly, coexpression of non-GFP–tagged w/t EphA3 with either nb-EphA3-GFP or [Phe_{152}-Leu] EphA3GFP effectively restored phosphorylation of nb-EphA3-GFP and its recruitment into large EphA3 clusters. The extensive FRET-positive area surrounding ephrin-A5-Fc beads demonstrates that cluster propagation does not rely on direct ephrin contact (Fig. 4 B). Intuitively, the role of preclustered ephrin lies in its ability to recruit neighboring receptors, which engage available Eph-binding sites according to the avidity of the ephrin aggregate. Although transgenic mouse studies (Brown et al., 2000) have provided in vivo support for this concept, the assembly mechanism of Eph–ephrin signaling clusters has remained unexplored. Our experiments indicate that, initiated by oligomeric ephrin, the propagation of Eph signaling clusters does not depend on ephrin contact but instead is governed by the receptors themselves.

We sought to assess a potential involvement of the EphA3 signaling function in this process, by immunoprecipitation analysis of HEK293T cells expressing combinations of GFP-tagged and nontagged w/t or nb-EphA3, in addition to signaling-impaired mutants lacking tyrosines (3YF EphA3; Lawrenson et al., 2002) or a functional ATP-binding site ([K_{653}-M] EphA3). After stimulation with preclustered ephrin-A5-Fc, ligand-bound receptor aggregates were recovered on protein A–Sepharose beads. In agreement with FRET analysis (Fig. 4 B), anti-GFP immunoblots revealed effective phosphorylation and coprecipitation of nb-EphA3-GFP receptors within the ephrin-A5–bound complex only when coexpressed with w/t receptor (Fig. 4 C). Importantly, also 3YF and [K_{653}-M] EphA3 mutants effectively recruited nb-EphA3, suggesting that neither EphA3 kinase activity nor the principle SH2 docking sites are required.

To explore the possible involvement of kinase and SH2 domain-independent functions of the EphA3 cytoplasmic domain, we performed the coprecipitation with EphA3Δcyto, a transmembrane mutant lacking the cytoplasmic domain (Fig. 4 D). Intriguingly, in EphA3Δcyto coexpressing cells, nb-

EphA3-GFP was effectively recruited and coprecipitated, suggesting that indeed extracellular receptor–receptor interactions facilitate the ephrin-independent propagation of Eph signaling clusters. This notion concurs with an earlier observation that a truncated EphA3 exodomain lacking the ephrin-binding domain facilitates EphA3 phosphorylation in vitro and acts as a dominant-negative inhibitor of EphA3 function in vivo (Lackmann et al., 1998).

Our findings have important implications for the understanding of Eph-mediated cell guidance. Eph-mediated but kinase-independent cell positioning has been described in several developmental programs (Boyd and Lackmann, 2001); EphA7 splice variants lacking kinase activity provide essential ephrin-A5 adhesion contacts during mouse neural fold closure, and coexpression of w/t and kinase-dead EphA7 switches cell contact repulsion to adhesion (Holmberg et al., 2000). Our data now reveal a mechanism that can recruit not only signaling-impaired but ephrin-binding compromised Ephs into the same signaling cluster. Therefore, Eph receptor clustering provides a simple mechanism to dynamically modulate a cellular response according to overall composition and abundance of receptor variants within a given cell. It will be interesting to examine if this mechanism also allows for the recruitment of different Eph RTK family members into the same cluster, and experiments to address this notion are ongoing.

The organization of transmembrane receptors into higher order signaling clusters is likely to be a universal biological communication mechanism and accounts for the finely graded responses of prokaryotic chemotaxis receptors (Gestwicki et al., 2000; Kim et al., 2002) and for ligand selectivity of T cell receptor complexes (Krummel and Davis, 2002). For ephrin-directed pathfinding, the current model suggests that migration of Eph-bearing cells into a gradient of ephrin expression is controlled by Eph receptor affinity and abundance and by competition for ephrin targets (Monschau et al., 1997; Brown et al., 2000; Feldheim et al., 2000). The clustering mechanism revealed by our findings is suited to exert this control, whereby nucleating oligomeric Eph–ephrin complexes will recruit a proportion of receptors into a signaling cluster that would represent the overall receptor abundance of the cell. Similar to bacterial chemotaxis mechanisms, this concept allows for precisely adjusted cellular responses controlled by graded changes in ligand abundance and receptor/ligand occupancy, a characteristic feature of Eph–ephrin communication.

Materials and methods

Expression constructs and reagents

Full-length w/t and mutant EphA3 containing tyrosine-to-phenylalanine substitutions of the three major phosphorylation sites (3YF EphA3; Lawrenson et al., 2002) were engineered to contain COOH-terminal EGFP (CLONTECH Laboratories, Inc.). Isolation and characterization of ephrin-binding compromised EphA3 mutants has been described previously (Smith et al., 2003). EphA3GFP with abrogated ephrin-A5 binding capacity (nb-EphA3-GFP) was generated by introducing (site-directed mutagenesis kit; Stratagene) substitutions Phe_{152}-to-Leu and Val_{133}-to-Glu within the putative EphA3 heterodimerization and heterotetramerization domains, respectively. A Lys_{653}→Met mutation was introduced within the EphA3 ATP-binding site to abrogate kinase activity; for EphA3Δcyto, a stop codon was inserted at Tyr_{570}. GFP ephrin-A2 (Hattori et al., 2000) was a gift from J. Flanagan (Harvard Medical School, Boston, MA). Expression plasmids (pIgBOS) encoding extracellular domains of ephrin-A5 or EphA3 (Coulthard et al., 2001) fusion proteins with the hinge and Fc region of human IgG1 (a gift from A. van der Merwe, Oxford University, Oxford, UK) were prepared, EphA3-Fc and ephrinA5-Fc were protein A affinity purified from culture supernatants of stable CHO transfectants. Monomeric ephrin-A5 was prepared as described previously (Lackmann et al., 1997).

Anti-EphA3 mAb, IIIA4, and affinity-purified rabbit polyclonal antibodies were described previously (Boyd et al., 1992; Lackmann et al., 1997). Other antibodies and reagents used were anti-GFP (Transduction Laboratories), 4G10 (Upstate Biotechnology), PY72 (Cancer Research UK), P-Tyr100 (New England Biolabs, Inc.), HRP-conjugated anti–mouse antibodies (Jackson ImmunoResearch Laboratories), HRP-conjugated anti–rabbit (Bio-Rad Laboratories), and rhodamine phalloidin and Lysotracker green (Molecular Probes).

Alexa Fluor 546 conjugates and polystyrene beads

Recombinant, purified ephrin-A5-Fc and EphA3-Fc were labeled with Alexa Fluor 546 (Molecular Probes). Coupling of the Alexa dye and its effect on the biological integrity of ephrin and Eph proteins were monitored by spectral (HPLC diode array detection) and BIAcore binding analysis. Binding to sensor chip-coupled EphA3 or ephrin-A5 (Lackmann et al., 1997, 1998) was used to monitor biological integrity. Alexa546 conjugates of EphA3 Fc and ephrin-A5-Fc (Alexa EphA3-Fc and Alexa ephrinA5-Fc) or unlabeled ephrin-A5-Fc were immobilized onto protein A–coated 5.6-μm polystyrene beads (Bangs Laboratories) according to the manufacturer's instructions. Ephrin-A5-Fc or Alexa ephrin-A5-Fc were preclustered (20 min) at a 1:10 molar ratio with anti–human Fc antibody (Jackson ImmunoResearch Laboratories) before experiments.

Cell culture

HEK293 (American Type Culture Collection) cells were maintained in DME, 10% FCS, and transfection of HEK293 cells was performed using Fugene 6 transfection reagent (Roche Biochemicals). Before each experiment, cells were serum starved in culture medium containing 0.5% FCS for at least 4 h. For live cell FRET microscopy experiments, the culture medium was replaced with CO_2-independent imaging medium.

Microscopy and immunocytochemistry

Immunocytochemistry and time-lapse confocal microscopy done on a microscope (model 1024; Bio-Rad Laboratories) using 60×, 1.4 NA oil (fixed cells, and 60×, 1.2 NA water (live cells) immersion lenses were performed as described previously (Lawrenson et al., 2002). Lysosomal cell compartments were stained with Lysotracker green (Molecular Probes). Images of green (Lysotracker CMFDA) and Alexa546 fluorescence were collected sequentially to minimize "bleed-through" from spectral overlap. Lysotracker was excited with the 488-nm line of a 100-mW argon ion laser (Ion Laser Technology) attenuated to 3% with a neutral density filter. Alexa546 was excited with the 514-nm argon laser line attenuated to 3% with a neutral density filter. For detection, 527 long pass primary and 565 long pass secondary dichroic mirrors, separating red and green fluorescence to separate detectors, and a narrow band barrier filter (522/35) were used.

GFP EphA3 (w/t or mutant) expressing cells were stimulated, fixed, permeabilized, and stained with Cy3-conjugated antiphosphotyrosine mAb PY72 before mounting onto glass slides using Mowiol (Calbiochem). Fluorescence lifetime imaging microscopy (FLIM) sequences were obtained at 80 MHz with a microscope (model IX70; Olympus; 100 /1.4 NA oil immersion lens) and analyzed as described previously (Reynolds et al., 2003). A 476-nm argon laser line and narrow-band emission filter (model HQ510/20; Chroma Technology Corp.) were used for GFP, a 100-W mercury arc lamp with high Q Cy3 filter set (excite, model HQ545/30; dicroic, model Q580LP; and emitter, model HQ610/75) was used for Cy3 and Alexa546. GFP Fluorescence was detected with a dichroic beamsplitter (model Q495 LP; Chroma Technology Corp.) and narrow band emission filter. FRET was measured in live 293 cells between transiently expressed ephrin-A2GFP and Alexa546 EphA3-Fc.

Immunoprecipitation and Western blotting

Serum-starved cells stimulated for 10 min with 1.5 μg/ml of preclustered ephrin-A5 were lysed as described previously (Lawrenson et al., 2002). Ephrin-A5–bound receptor clusters were precipitated with protein A–Sepharose (Amersham Biosciences) for at least 1 h at 4°C. Lysates and washed immunoprecipitates were analyzed by Western blot with appropriate antibodies and visualized using an ECL substrate (Pierce Chemical Co.).

Online supplemental material

The dynamics of ephrin-A5–binding to cell surface EphA3 and subsequent assembly of Eph-A3–ephrin-A5 signalling clusters was recorded in real-

time by time-lapse confocal microscopy and is illustrated in Video 1. Fig. S1 illustrates the formation of Eph–ephrin contacts that were monitored by fluorescence lifetime imaging using GFP ephrin-A2–expressing cells exposed to Alexa EphA3-Fc–coated beads and micrographs of salient time points. We examined the authenticity of FRET in our experiments by monitoring GFP fluorescence lifetimes in EphA3-GFP–expressing cells after CY3 photobleaching (Fig. S2, A and B) or in the absence of the fluorescence acceptor CY3-PY72 (Fig. S2 C). Online supplemental material is available at http://www.jcb.org/cgi/content/full/jcb.200312001/DC1.

We thank Peter Verveer, Christian Tischer, and Martin Offterdinger for help with FRET; Stephen Cody for confocal microscopy advice; and Giovanna d'Abacco for preparation of EphA3 mutants.

This work was supported by Melbourne University International Research, Abroad Traveling and *Journal of Cell Science* Traveling Fellowships (to S.H. Wimmer-Kleikamp), and National Health and Medical Research Council (grant 234707) and Anti-Cancer Counsel of Victoria (grant 62/2002) funding (to M. Lackmann).

Submitted: 1 December 2003
Accepted: 12 January 2004

References

Bastiaens, P.I., and R. Pepperkok. 2000. Observing proteins in their natural habitat: the living cell. *Trends Biochem. Sci.* 25:631–637.

Boyd, A.W., and M. Lackmann. 2001. Signals from Eph and ephrin proteins: a developmental tool kit. *Sci STKE.* 2001:RE20.

Boyd, A.W., L.D. Ward, I.P. Wicks, R.J. Simpson, E. Salvaris, A. Wilks, K. Welch, M. Loudovaris, S. Rockman, and I. Busmanis. 1992. Isolation and characterization of a novel receptor-type protein tyrosine kinase (hek) from a human pre-B cell line. *J. Biol. Chem.* 267:3262–3267.

Brown, A., P.A. Yates, P. Burrola, D. Ortuno, A. Vaidya, T.M. Jessell, S.L. Pfaff, D.D. O'Leary, and G. Lemke. 2000. Topographic mapping from the retina to the midbrain is controlled by relative but not absolute levels of EphA receptor signaling. *Cell.* 102:77–88.

Coulthard, M.G., J.D. Lickliter, N. Subanesan, K. Chen, G.C. Webb, A.J. Lowry, S. Koblar, C.D. Bottema, and A.W. Boyd. 2001. Characterization of the Epha1 receptor tyrosine kinase: expression in epithelial tissues. *Growth Factors.* 18:303–317.

Davis, S., N.W. Gale, T.H. Aldrich, P.C. Maisonpierre, V. Lhotak, T. Pawson, M. Goldfarb, and G.D. Yancopoulos. 1994. Ligands for EPH-related receptor tyrosine kinases that require membrane attachment or clustering for activity. *Science.* 266:816–819.

Feldheim, D.A., Y.I. Kim, A.D. Bergemann, J. Frisen, M. Barbacid, and J.G. Flanagan. 2000. Genetic analysis of ephrin-A2 and ephrin-A5 shows their requirement in multiple aspects of retinocollicular mapping. *Neuron.* 25: 563–574.

Flanagan, J.G., and P. Vanderhaeghen. 1998. The ephrins and Eph receptors in neural development. *Annu. Rev. Neurosci.* 21:309–345.

Gestwicki, J.E., L.E. Strong, and L.L. Kiessling. 2000. Tuning chemotactic responses with synthetic multivalent ligands. *Chem. Biol.* 7:583–591.

Hattori, M., M. Osterfield, and J.G. Flanagan. 2000. Regulated cleavage of a contact-mediated axon repellent. *Science.* 289:1360–1365.

Himanen, J.P., and D.B. Nikolov. 2003. Eph signaling: a structural view. *Trends Neurosci.* 26:46–51.

Himanen, J.P., K.R. Rajashankar, M. Lackmann, C.A. Cowan, M. Henkemeyer, and D.B. Nikolov. 2001. Crystal structure of an Eph receptor-ephrin complex. *Nature.* 414:933–938.

Holder, N., and R. Klein. 1999. Eph receptors and ephrins: effectors of morphogenesis. *Development.* 126:2033–2044.

Holmberg, J., D.L. Clarke, and J. Frisen. 2000. Regulation of repulsion versus adhesion by different splice forms of an Eph receptor. *Nature.* 408:203–206.

Kim, S.H., W. Wang, and K.K. Kim. 2002. Dynamic and clustering model of bacterial chemotaxis receptors: structural basis for signaling and high sensitivity. *Proc. Natl. Acad. Sci. USA.* 99:11611–11615.

Klein, R. 1999. Bidirectional signals establish boundaries. *Curr. Biol.* 9:R691–R694.

Krummel, M.F., and M.M. Davis. 2002. Dynamics of the immunological synapse: finding, establishing and solidifying a connection. *Curr. Opin. Immunol.* 14: 66–74.

Lackmann, M., R.J. Mann, L. Kravets, F.M. Smith, T.A. Bucci, K.F. Maxwell, G.J. Howlett, J.E. Olsson, T. Vanden Bos, D.P. Cerretti, and A.W. Boyd. 1997. Ligand for EPH-related kinase (LERK) 7 is the preferred high affinity ligand for the HEK receptor. *J. Biol. Chem.* 272:16521–16530.

Lackmann, M., A.C. Oates, M. Dottori, F.M. Smith, C. Do, M. Power, L. Kravets, and A.W. Boyd. 1998. Distinct subdomains of the EphA3 receptor mediate ligand binding and receptor dimerization. *J. Biol. Chem.* 273: 20228–20237.

Lawrenson, I.D., S.H. Wimmer-Kleikamp, P. Lock, S.M. Schoenwaelder, M. Down, A.W. Boyd, P.F. Alewood, and M. Lackmann. 2002. Ephrin-A5 induces rounding, blebbing and de-adhesion of EphA3-expressing 293T and melanoma cells by CrkII and Rho-mediated signalling. *J. Cell Sci.* 115: 1059–1072.

Monschau, B., C. Kremoser, K. Ohta, H. Tanaka, T. Kaneko, T. Yamada, C. Handwerker, M.R. Hornberger, J. Loschinger, E.B. Pasquale, et al. 1997. Shared and distinct functions of RAGS and ELF-1 in guiding retinal axons. *EMBO J.* 16:1258–1267.

Ostman, A., and F.D. Bohmer. 2001. Regulation of receptor tyrosine kinase signaling by protein tyrosine phosphatases. *Trends Cell Biol.* 11:258–66.

Reynolds, A.R., C. Tischer, P.J. Verveer, O. Rocks, and P.I. Bastiaens. 2003. EGFR activation coupled to inhibition of tyrosine phosphatases causes lateral signal propagation. *Nat. Cell Biol.* 5:447–453.

Smith, F.M., C. Vearing, M. Lackmann, H. Treutlein, J.P. Himanen, K. Chen, A. Saul, D.B. Nikolov, and A.W. Boyd. 2003. Dissecting the EphA3/ephrin-A5 interactions using a novel functional mutagenesis screen. *J. Biol. Chem.* 10.1074/jbc.M309326200.

Stein, E., A.A. Lane, D.P. Cerretti, H.O. Schoecklmann, A.D. Schroff, R.L. Van Etten, and T.O. Daniel. 1998. Eph receptors discriminate specific ligand oligomers to determine alternative signaling complexes, attachment, and assembly responses. *Genes Dev.* 12:667–678.

Wouters, F.S., P.J. Verveer, and P.I. Bastiaens. 2001. Imaging biochemistry inside cells. *Trends Cell Biol.* 11:203–211.